Check for updates

ACES Asian Chemical Editorial Society

DOI: 10.1002/asia.202100060

CHEMISTRY AN ASIAN JOURNAL Full Paper

VIP

Improved Stabilities of Labeling Probes for the Selective Modification of Endogenous Proteins in Living Cells and In Vivo

Kuan-Yu Lin[+],[a] Chak Hin Lam[+],[a] Xin-Hui Lin,[a] Jung-I Hsu,[a] Syuan-Yun Fan,[a] Nitesh K. Gupta,[a] Yu-Chun Lin,[a] Boon Khoon Tee,[a] Jui-Ping Li,[d] Jen-Kun Chen,[d] and Kui-Thong Tan*[a, b, c]

Abstract: To date, various affinity-based protein labeling probes have been developed and applied in biological research to modify endogenous proteins in cell lysates and on the cell surface. However, the reactive groups on the labeling probes are also the cause of probe instability and nonselective labeling in a more complex environment, e.g., intracellular and in vivo. Here, we show that labeling probes composed of a sterically stabilized difluorophenyl pivalate can achieve efficient and selective labeling of endogenous proteins on the cell surface, inside living cells and in vivo. As compared with the existing protein labeling probes, probes with the difluorophenyl pivalate exhibit several advantages, including long-term stability in stock solutions, resistance to enzymatic hydrolysis and can be customized easily with diverse fluorophores and protein ligands. With this probe design, endogenous hypoxia biomarker in living cells and nude mice were successfully labeled and validated by in vivo, ex vivo, and immunohistochemistry imaging.

Introduction

Protein modification with small molecules is an important strategy to realize many biological and medical applications, including the protein imaging in complex biological systems, functional studies of individual proteins, and development of new biopharmaceuticals.[1] To achieve selective chemical modification of target proteins in complex biological contexts, e.g., cells, tissues and animals, most strategies rely on protein/peptide tags and bioorthogonal chemistry-based methods.[2] Although these approaches are versatile and robust, the major limitation is that they are only applicable to genetically-encoded proteins, and cannot be used directly to study endogenous proteins in living cells and in vivo.

In contrast, the chemical modification of the target protein using affinity-based protein labeling probes can provide an opportunity to detect and study endogenous proteins in the crowded and multimolecular cellular environments. In a typical design, the probe binds to the protein of interest (POI) via a specific protein-ligand interaction, triggering a chemical reaction via the proximity effect between the reactive group and an amino acid near the binding site of the POI. To date, a variety of chemically and photochemically reactive electrophiles have been incorporated in the affinity-based protein labeling probes, including activated esters, sulfonyl chlorides, epoxides, maleimides and α-halocarbonyls, as well as photo-activatable groups, such as aryl azide, diazirin, and benzophenone.[3] In addition to these reactive modules, Hamachi and co-workers have also developed several cleavable electrophiles to create ligand-directed traceless labeling probes. In this approach, the ligand can be easily released from the binding site of the POI upon labeling to allow the POI to retain its native activity and function. Several other electrophiles have been employed in the traceless labeling probes, including tosyl, acyl imidazole, dibromophenyl benzoate, *N*-sulfonyl pyridone, and *N*-acyl-*N*-alkyl sulfonamide.[4] Although these reactive moieties are valuable for the development of protein labeling probes for protein imaging, proteomics analysis, irreversible inhibition of protein activity, and biosensor construction, the reactive nature of such electrophiles is also the root cause of many selectivity and stability problems with these probes.[5]

Ideally, biocompatible electrophiles exhibiting fast reaction are desirable for efficient protein labeling. However, such high reactivity may produce significant nonspecific reactions due to the complex nature of biological systems. Therefore, despite the success of several affinity-based protein labeling probes for the modification of endogenous proteins in live cells, covalent modification of in vivo endogenous proteins remains a formidable task and have yet to be applied directly for endogenous protein of tumor cells in living animals.

In this paper, we report a novel phenyl ester moiety based on a bulky difluorophenyl pivalate electrophile to create sterically stabilized and highly selective affinity-based traceless protein labeling probes for the covalent modification of

[a] *K.-Y. Lin,[+] C. Hin Lam,[+] X.-H. Lin, J.-I Hsu, S.-Y. Fan, Dr. N. K. Gupta, Y.-C. Lin, B. Khoon Tee, Prof. Dr. K.-T. Tan*
Department of Chemistry, National Tsing Hua University, 101 Section 2, Kuang Fu Road, Hsinchu 30013 (Taiwan)
E-mail: kttan@mx.nthu.edu.tw

[b] *Prof. Dr. K.-T. Tan*
Frontier Research Center on Fundamental and Applied Sciences of Matters, National Tsing Hua University, 101 Section 2, Kuang Fu Road, Hsinchu 30013 (Taiwan)

[c] *Prof. Dr. K.-T. Tan*
Department of Medicinal and Applied Chemistry, Kaohsiung Medical University, Kaohsiung 807 (Taiwan)

[d] *J.-P. Li, Dr. J.-K. Chen*
Institute of Biomedical Engineering and Nanomedicine, National Health Research Institutes, Miaoli 35053 (Taiwan)

[+] *These authors contributed equally.*

Supporting information for this article is available on the WWW under https://doi.org/10.1002/asia.202100060

© 2021 Wiley-VCH GmbH

endogenous proteins in living cells and in vivo (Figure 1). The phenyl esters can potentially modify lysine residues, which occurs abundantly on protein surfaces and are nucleophilic enough under physiological conditions. Previously, several fluorescent probes based on phenyl ester have been applied in the labeling of different protein targets.[4c,6] Despite their high selectivity, the phenyl ester probes degraded rapidly in the presence of esterase and were prone to hydrolysis. For broader protein labeling applications, the phenyl ester probe must exhibit both sufficient labeling and resistance to the catalytic- and auto-hydrolysis in a complex environment, e.g. intracellular and in vivo conditions.

Herein, we show that our design for an affinity-based protein labeling probe based on a difluorophenyl pivalate electrophile (Figure 2a and Figure 4a) can be customized easily with various fluorophores and ligands to label selectively and efficiently different target proteins, e.g. carbonic anhydrase (CA), avidin and *E.coli* dihydrofolate reductase (eDHFR), in cell lysates, living cells and living animals. Our probes exhibit long term stability in aqueous buffer and stock solutions as well as resistance to catalytic hydrolysis by esterase. Besides the labeling of endogenous proteins in intracellular and in vivo environments, we also showed that the difluorophenyl pivalate probes can be used to quantify endogenously expressed cell surface hCAIX and hCAXII proteins under normoxia and hypoxia conditions.

Results and Discussion

Molecular design and reactivity of the affinity-based phenyl ester probes

The use of phenyl ester as a cleavable electrophilic group allows the stability and reactivity of the probe to be optimized at the phenol and the carboxylate sites, respectively. We sought to modulate the reactivity of the probe by introducing ortho-substituted dihalogen phenols as good leaving groups (Figure 2a, R_1=H, F, Cl and Br). Since the reported experimental pKa values of phenol, ortho-difluorophenol, ortho-dichlorophenol and ortho-dibromophenol are 9.9, 7.51, 6.78 and 6.67, respectively, the probe reactivity should increase as the pKa of the phenol decreases.[7] The stability was further optimized by using a sterically hindered pivalate moiety to minimize autolysis and enzymatic hydrolysis. Based on this principle, we designed five different probes **1–5** containing a sulfonamide ligand and a synthetic fluorescein dye. Human carbonic anhydrase II (hCAII) and sulfonamide were chosen as the initial target-ligand pair because their binding is known to be highly specific with K_i value of about 260 nM.[8] The synthesis of probes **1–5** can be accomplished in 7 steps, where the final step involves the coupling of the sulfonamide ligand via Huisgen 1,3-dipolar cycloaddition (Scheme S1–S9). This synthetic design facilitates the rapid and simple interchange of the ligand for the labeling of other target proteins in the future.

To examine which probe is the most effective for the labeling of hCAII, the labeling reactions of probes **1–5** (5 μM) and purified recombinant hCAII (5 μM) were conducted and analyzed by SDS-PAGE in-gel fluorescence and coomassie brilliant blue staining. As shown in Figure 2b, fluorescence was clearly observed from the bands for hCAII (MW ~ 32KDa, Figure S1) after a 2 hours incubation with **2** and **3**, whereas weak fluorescence were observed with **1**, **4** and **5**. The fluorescence intensity was reduced dramatically when a competitive inhibitor of hCAII, ethoxzolamide (EZA) was added, indicating that these labeling reactions were driven by a specific ligand-protein interaction. In contrast to **2** and **3**, the fluorescent bands for **1**, **4** and **5** remained very weak even after 4 hours of incubation.

The protein labeling level by each of the five probes was quantified by measuring the mean fluorescence intensity of the bands pixel-by-pixel using ImageJ software. The results showed that the least sterically hindered **2** is the most efficient at labeling hCAII. Based on the fluorescence intensity generated by **2**, about 40% and 60% of hCAII were labeled by **3** after 2 and 4 hours incubation. Comparatively, the hCAII protein labeling levels for **1**, **4** and **5** were merely 2%, 6%, and 3% after

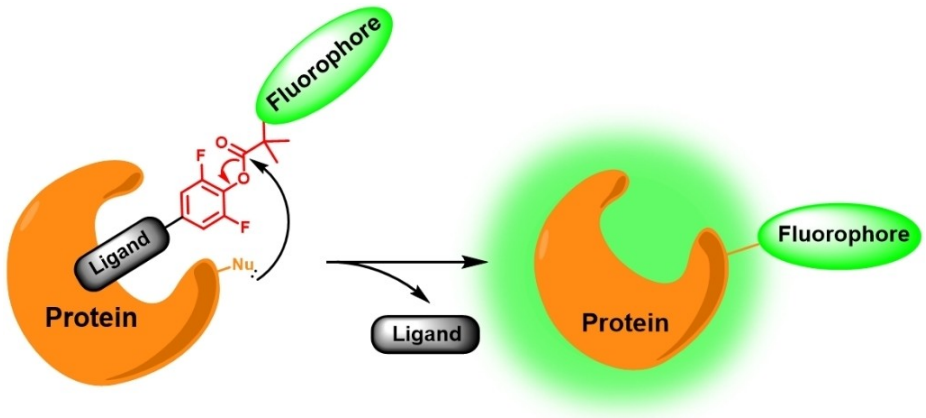

Figure 1. Schematic illustration of an affinity-based traceless protein labeling probe based on the difluorophenyl pivalate activated ester as a reactive electrophile. In the presence of a specific protein-ligand interaction, an acylation reaction between the difluorophenyl pivalate group and an amino acid near the active pocket of the target protein can occur via proximity effect.

© 2021 Wiley-VCH GmbH

(a)

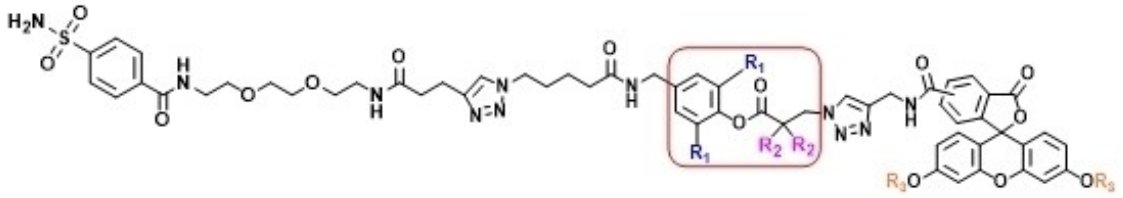

Probes	1	2	3	4	5	3[OAc]$_2$
R_1	H	F	F	Cl	Br	F
R_2	Me	H	Me	Me	Me	Me
R_3	H	H	H	H	H	Ac

(b)

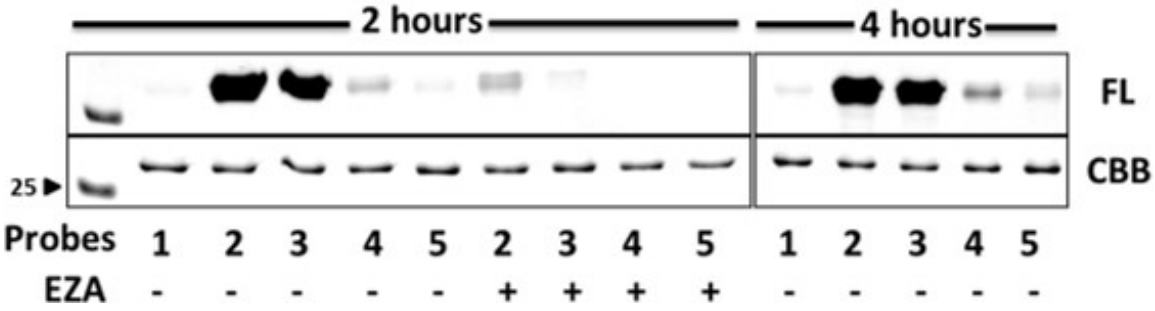

Figure 2. Molecular design and reactivity analyses of the affinity-based phenyl ester probes to label hCAII protein. (a) Chemical structures of protein labeling probes **1–5** for hCAII containing sulfonamide ligand and fluorescein dye. (b) Analysis of the covalent labeling of purified hCAII with **1–5**. Reaction conditions: hCAII (5 μM) and labeling probes (5 μM) were incubated in the absence or presence of 100 μM EZA in PBS buffer (pH 7.4) at 37 °C. The gel was analyzed by in-gel fluorescence imaging and stained with Coomassie brilliant blue (CBB).

4 hours of reaction. In general, the reactivity of the probes increases with decreasing steric hindrance (e.g. **2** and **3**) and pKa values of the phenol leaving groups (e.g. **1** and **3**). However, the impact of lower pKa values on probe reactivity can be offset by the increased steric hindrance caused by the larger molecular size of chloro and bromo atoms (the CPK model is shown in Figure S2). Thus, the difluorophenyl ester moiety on **2** and **3** provides a good balance between electrophilicity and steric hindrance to accomplish efficient protein labeling. We also confirmed that the labeling of hCAII with the phenyl ester probes occurs in a traceless manner by using activity assay and MALDI-TOF MS analysis. In the activity assay, we found that the enzymatic activity of hCAII to hydrolyze *p*-nitrophenol acetate was not affected after labeling with **2** (Figure S3). As for the MALDI-TOF MS analysis, we were able to observe the molecular peak of the released sulfonamide ligand upon labeling of hCAII with **2** and **3** (Figure S4). From the previous results, we believe that the labeling sites for hCAII by probe **3** should also occur at Lys 190 and 192, respectively.[6b]

Stability, labeling kinetic and selectivity of the affinity-based difluorophenyl pivalate probes

Maintaining the chemical integrity of small molecule probes in stock solutions for long-term storage and freeze/thaw cycles is a fundamental concern for the reproducibility of the results. It is known that a certain proportion of chemical compounds decompose over time when stored in DMSO, which is the most common solvent employed.[9] To this end, we investigated the stabilities of **2** and **3** stored in DMSO by HPLC analysis. The results from the HPLC chromatogram showed that **3** can maintain up to 98% purity after 12 months of storage in DMSO (1 mM) at −80 °C with no signs of degradation (Figure 3a and Figure S5). Furthermore, **3** was also stable in MeOH or to be stored as a dry form at −80 °C for at least 18 months (Figure S6). On the other hand, **2** decomposed slowly in DMSO, leaving with only 90% purity after 4 months of storage at −80 °C (Figure S7). In comparison, activated esters that are based on *N*-hydroxysuccinimide (NHS, pKa = 6.0) and pentafluorophenol (pKa = 5.5) are not stable in aqueous buffer and DMSO solvent.[10]

Next, we evaluated the stabilities of **2** and **3** under the labeling conditions and in the presence of esterase. Through HPLC analysis, we determined that only 6% of **2** and 3% of **3**

© 2021 Wiley-VCH GmbH

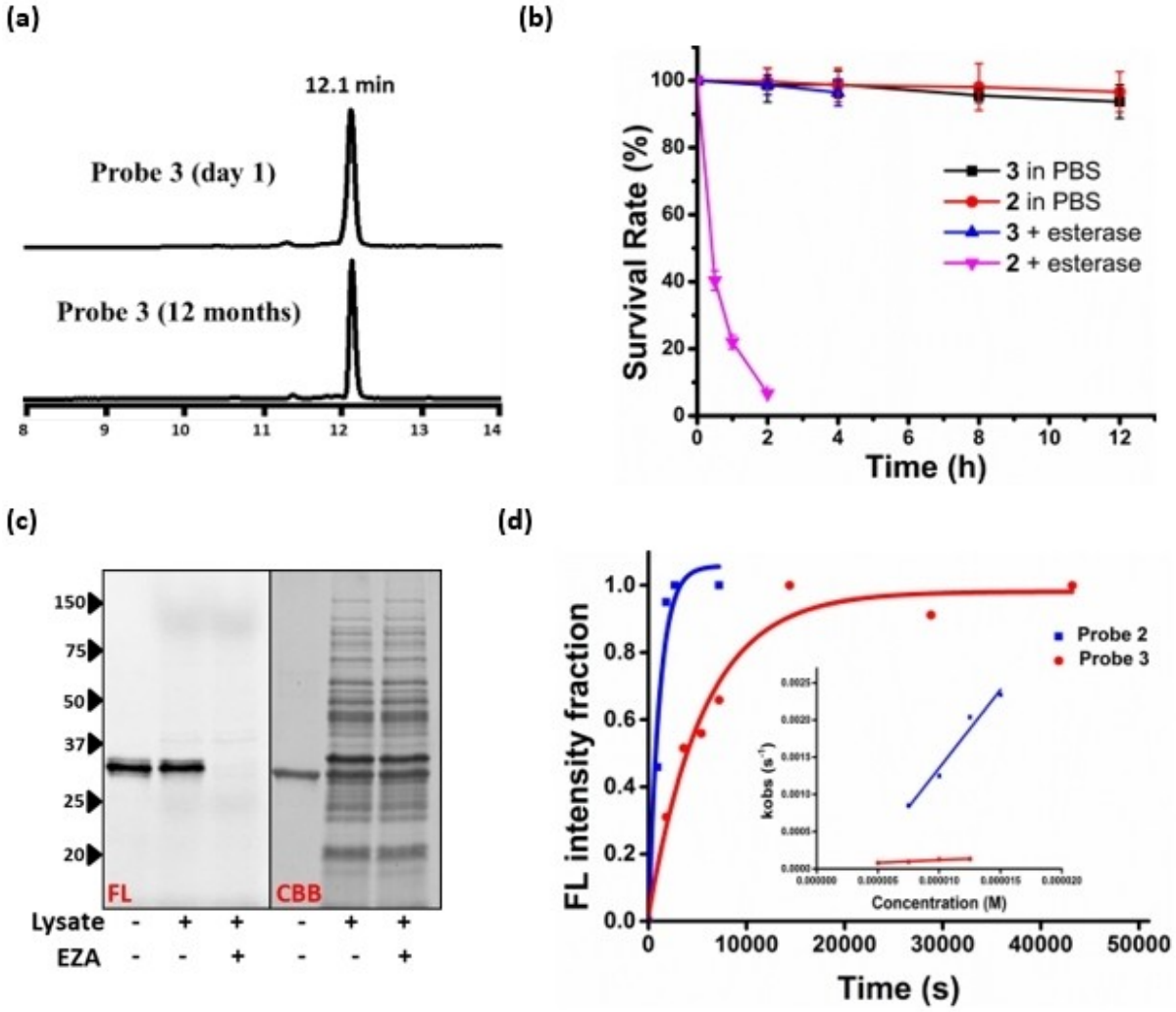

Figure 3. Stability, labeling kinetic and selectivity of **2** and **3**. (a) HPLC trace of **3** on day 1 and after storage in DMSO at −80 °C for 12 months. (b) HPLC trace analyses of **2** and **3** in the absence or presence of PLE (330 nM) in pH 7.4 PBS buffer at 37 °C. Error bars were calculated from three measurements. (c) SDS-PAGE analysis of hCAII labeling with 5 μM **3** in 6 mg/mL *E. coli* lysates at 37 °C for 2 hours. (d) Time course of fluorescence increase for the reaction of hCAII (2.5 μM each) with **2** and **3** (25 μM each) at 37 °C in pH 7.4 PBS buffer. The inset shows the kinetic plot of the apparent reaction rate constant k_{obs} (s^{-1}) versus various concentrations of **2** and **3** ($R^2 = 0.99$).

were hydrolyzed after 12 hours of incubation at 37 °C in PBS buffer (Figure 3b and Figure S8). While **2** and **3** exhibit similar stabilities under the labeling condition, their resistances to hydrolysis by esterase are completely dissimilar. Upon the addition of 330 nM (~1 U/mL) porcine liver esterase (PLE), **2** decomposed completely after 2 hours, whereas 96% of **3** remained after 4 hours of incubation (Figure S9). The ability of **3** to resist catalytic hydrolysis by PLE prompted us to investigate the efficiency of **3** to label hCAII under high concentrations of PLE (Figure S10). The results showed that even in the presence of 10 μM PLE, **3** can still achieve about 80% of hCAII labeling. As PLE is a reactive esterase with high catalytic efficiency ($k_{cat}/K_m = 1 \times 10^6\ M^{-1}s^{-1}$ for fluorescein diacetate), these results also suggest that the probe should be able to resist catalytic hydrolysis by intracellular and in vivo esterase.[11] Taken together, we believe that the high stability of the probe in DMSO stock solution and in the presence of esterase is due to the synergetic effect of the difluorophenol's moderate pK_a value (pKa = 7.51) and the bulky pivalate group.

Having optimized probe **3** as a highly stable labeling reagent, we attempted to evaluate its protein labeling selectivity under crude conditions. The labeling reactions were carried out with 5 μM **3** using cell lysates of *E. coli* (6 mg/mL) with overexpressed hCAII (Figure 3c). A clear single fluorescent band corresponding to hCAII appeared when the purified hCAII and lysates were incubated with **3**, which was not visible in the presence of EZA. Although **2** is more efficient in labeling its target protein, it also suffers from significant levels of non-specific labeling in the crude mixture (Figure S11). In fact, this problem is prevalent among protein labeling probes which employed highly reactive electrophiles. Therefore, probe **3** which is based on the difluorophenyl pivalate moiety offers an optimal balance between reactivity and selectivity to label the target protein in complex biological environments.

© 2021 Wiley-VCH GmbH

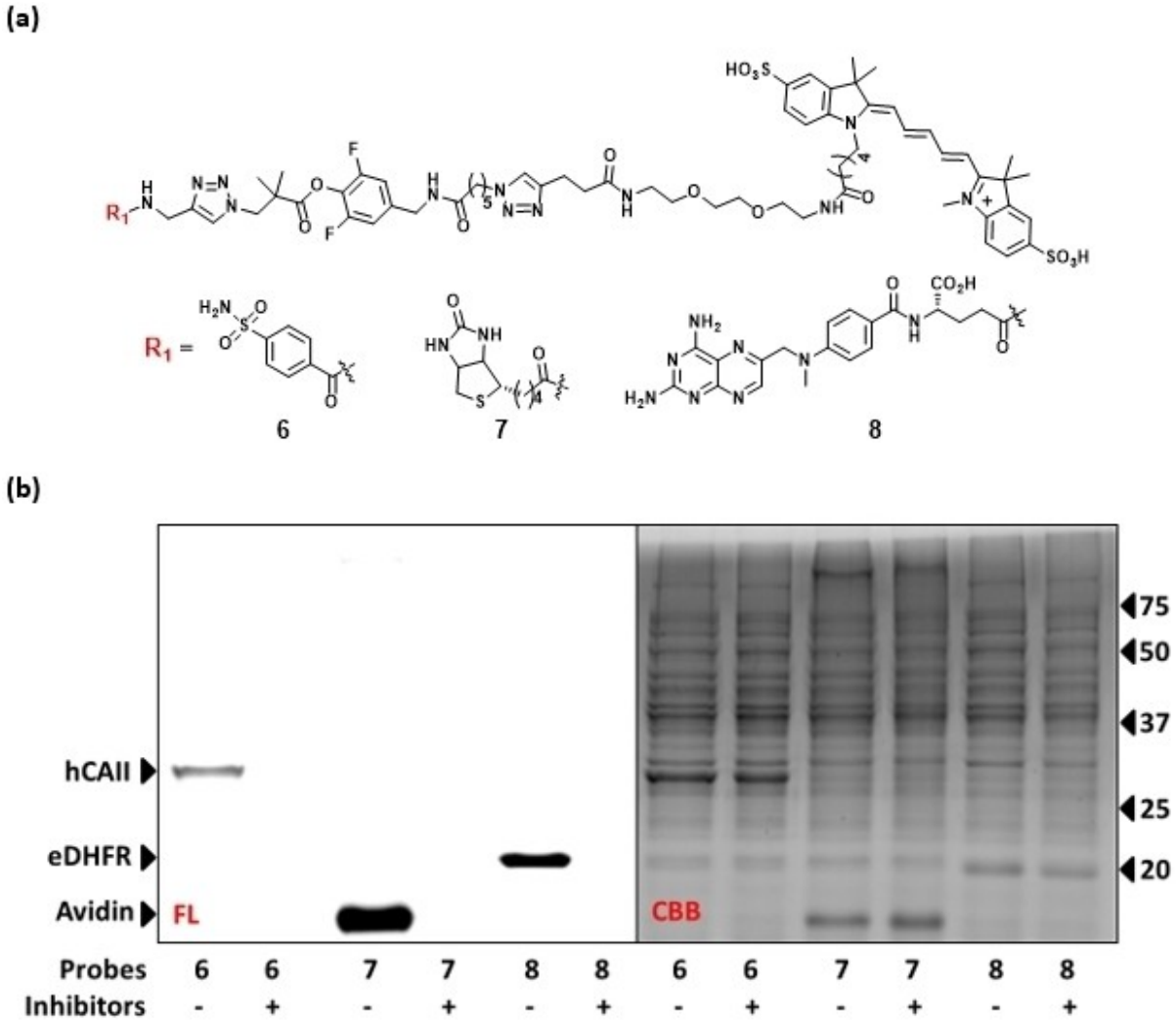

Figure 4. (a) Chemical structures of protein labeling probes **6**, **7** and **8** which are used for the labeling of hCAII, avidin and eDHFR, respectively. (b) SDS-PAGE in-gel fluorescent analysis of the covalent labeling of hCAII, avidin and eDHFR (5 μM each) with equal concentration of **6**, **7** and **8**, respectively, in 5 mg/mL *E. coli* lysates at 37 °C for 2 hours. EZA, biotin and methotrexate (100 μM each) were used as an inhibitor for inhibiting covalent labeling of hCAII, avidin and eDHFR, respectively.

To better understand the high stability and selectivity of **3** to label hCAII under esterase and lysate conditions, kinetic analyses of the labeling reactions with hCAII were carried out by monitoring the increase of fluorescence intensity over time at SDS-PAGE gel (Figure S12). As expected, the less sterically hindered **2** exhibits faster labeling kinetic with hCAII, achieving full labeling within 1 hour (Figure 3d). For **3**, full labeling was accomplished after 6 hours of reaction. The second-order rate constants (k_2) for **2** and **3** were determined to be about 210 and 7.4 $M^{-1}s^{-1}$, respectively (Figure 3d, inset). With the given k_2 values, the reaction rate of difluorophenyl pivalate is comparable to the copper-catalyzed azide-alkyne cycloaddition as well as LDAI and LDT chemistry developed by Hamachi and coworkers.[3a,12] It is significant to note that with this labeling rate, difluorophenyl pivalate protein probes are able to label very low amounts of target protein, achieving protein detection limit of around 1 ng (Figure S13). We also found that the reaction kinetic is correlated with the binding affinity between the ligand and the target protein. Due to the existence of a weak binding between sulfonamide and BSA (K_d ~ 1–10 μM), the k_2 value of **3** with BSA was determined to be around 0.70 $M^{-1}s^{-1}$ which is about 10 times smaller than the reaction with hCAII (Figure S14).[13] This indicates that difluorophenyl pivalate probes can also be used to label proteins with weak binding affinity.

Traceless labeling of hCAII, avidin and eDHFR proteins in cell lysates

To show the modular nature of our difluorophenyl pivalate probe design, we replaced the fluorescein and sulfonamide with the probes that contain Cy5 dye and various other ligands, e.g. sulfonamide, biotin and methotrexate, to generate probe **6**, **7**, and **8** for the labeling of recombinant hCAII, avidin (MW ~ 16KDa, monomer) and recombinant *E.coli* dihydrofolate reduc-

© 2021 Wiley-VCH GmbH

tase (eDHFR, MW ~ 21KDa) proteins, respectively (Figure 4a). To evaluate the protein labeling of the probes under crude conditions, hCAII, avidin and eDHFR (5 μM each) were reacted with equal concentration of **6**, **7** and **8**, respectively, in *E. coli* lysates (5 mg/mL) at 37 °C for 2 hours. As shown in Figure 4b, a clear single fluorescent band was observed for the target protein which was not visible in the presence of the corresponding inhibitor. To further validate the high selectivity of the difluorophenyl pivalate probes in a medium containing high protein concentration, we applied the protein labeling strategy in fetal bovine serum (FBS) which has about 56 mg/mL of total proteins as determined by BCA assay. The results showed that as little as 6.25 ng of hCAII and 13 ng of avidin can be labeled and detected in FBS (Figure S15). A similar detection limit can be obtained when the labeling reaction was performed in clean PBS buffer, indicating the consistent and reliable performance of the probe to label target protein in different environments (Figure S16). Due to the existence of a weak binding between sulfonamide and BSA, labeling of BSA can be observed when the amount of hCAII in FBS was low (Figure S17). These results show that the difluorophenyl pivalate moiety is a robust electrophile that can be easily modified by incorporating different ligands and fluorescent dyes, and can also be applied to mediums containing high concentration of proteins.

Labeling, imaging and identification of basal extracellular carbonic anhydrase isozymes

Carbonic anhydrases (CAs) form a family of enzymes that catalyze the inter-conversion between carbon dioxide and carbonic acid.[8] Depending on tissue distribution, cellular localization and conditions, the role of the enzyme changes slightly. For example, transmembrane-type human carbonic anhydrase IX (hCAIX, ~ 50 kDa) and XII (hCAXII, ~ 44 kDa) are highly expressed under hypoxia condition in many tumor cell lines.[14] Tumor hypoxia is linked with reduced efficacy of cancer therapies which makes the two CAs valuable biomarkers for preclinical and diagnostic imaging.[15] Currently, western blot analysis is the standard method used to detect and identify the different CA isozymes. We believe that the identity of extracellular CA isozymes can be rapidly revealed by labeling the proteins with either **6** or **3**, followed by molecular weight identification using in-gel fluorescent imaging, thereby avoiding the laborious western-blot analysis.

To show that our difluorophenyl pivalate probes are sufficiently sensitive and selective to detect endogenous proteins in living cells, **3** was applied for the imaging and identification of basal transmembrane CA isozyme of MCF7 and A549 cells under normoxia conditions. We first applied cell-impermeable **3** to demonstrate the utility of the probe in imaging extracellular carbonic anhydrases of MCF7 and A549 cells cultured under normoxia conditions. When the cells were treated with **3**, strong fluorescence along the surface of MCF7 and A549 cells was observed (Figure 5a). In contrast, negligible fluorescence was observed when EZA was added to the cells. This imaging result was validated by labeling HeLa cells that overexpress transmembrane CFP-hCAII protein with probe **6** (Figure S18). The fluorescence from the Cy5 channel overlaid very well with the CFP-hCAII protein expressed on the cell surface. To characterize the extracellular CA isozymes of MCF7 and A549, the cells labeled with **3** were lysed and identified by in-gel fluorescence analysis. The results showed that two distinct fluorescent bands at ~ 50 kDa and ~ 44 kDa can be observed clearly from the cell lysates of MCF7 and A549 cells (Figure 5b and Figure S19). As the bands were not visible in the presence of EZA, this indicates that the labeling by **3** is specific for CA isozymes. We believe that the slower reactivity of difluorophenyl pivalate group and the highly selective interaction of sulfonamide ligand with CA proteins are important factors for the specific labeling in living cells. In line with the in-gel fluorescence results, significant western-blot bands were observed for MCF7 with anti-hCAIX antibody and for A549 with anti-hCAXII (major band) and anti-hCAIX (minor band) antibodies (Figure 5c). These results correlate with many previous reports which indicate that the major basal extracellular CA isozymes under normoxia conditions for MCF7 and A549 cells are hCAIX and hCAXII, respectively.[14b,d] It is also important to note that dual-color imaging of hCAIX protein can be accomplished when **3** and **6** were added sequentially to MCF7 cells (Figure S20). This indicates that the difluorophenyl pivalate probe can be a very useful protein labeling toolkit for biological experiments that require double protein labeling to unveil accurate and precise insights.

Imaging, labeling and quantification of hypoxia-induced carbonic anhydrase isozymes

To further demonstrate the importance of difluorophenyl pivalate as a reactive module in protein labeling and biological applications, **3** was used to label overexpressed extracellular CAs of A549 cells under hypoxia conditions. To induce the overexpression of CAs, A549 cells were cultured in the presence of 200 μM $CoCl_2$ for 24 hours to mimic the hypoxia.[16] When **3** was added to the hypoxia-mimetic A549 cells, strong fluorescence along the cell surface was observed as compared to the cells cultured under normoxia (Figure 6a). The **3**-labeled A549 cells were subsequently lysed and analyzed by in-gel fluorescence to identify the type of overexpressed extracellular CA isozymes (Figure 6b). The results showed that the expression level of hCAXII under the hypoxia-mimetic condition was increased by about 33% (Figure 6c). As a comparison, western-blot analysis also showed that hypoxia-A549 cells expressed about 30% higher level of hCAXII (Figure S21).

It is noteworthy to mention that the minor hCAIX protein of A549 cells can also be detected if probe **6**, with a brighter Cy5 dye, was used to label the cells (Figure S22). The in-gel fluorescence analysis of the **6**-labeled A549 cells showed that the expression level for hCAIX and hCAXII under hypoxia-mimetic conditions were increased by about 68% and 35%, respectively. These results indicate that the expression of hCAIX in A549 cells is more sensitive to the hypoxia condition, which

© 2021 Wiley-VCH GmbH

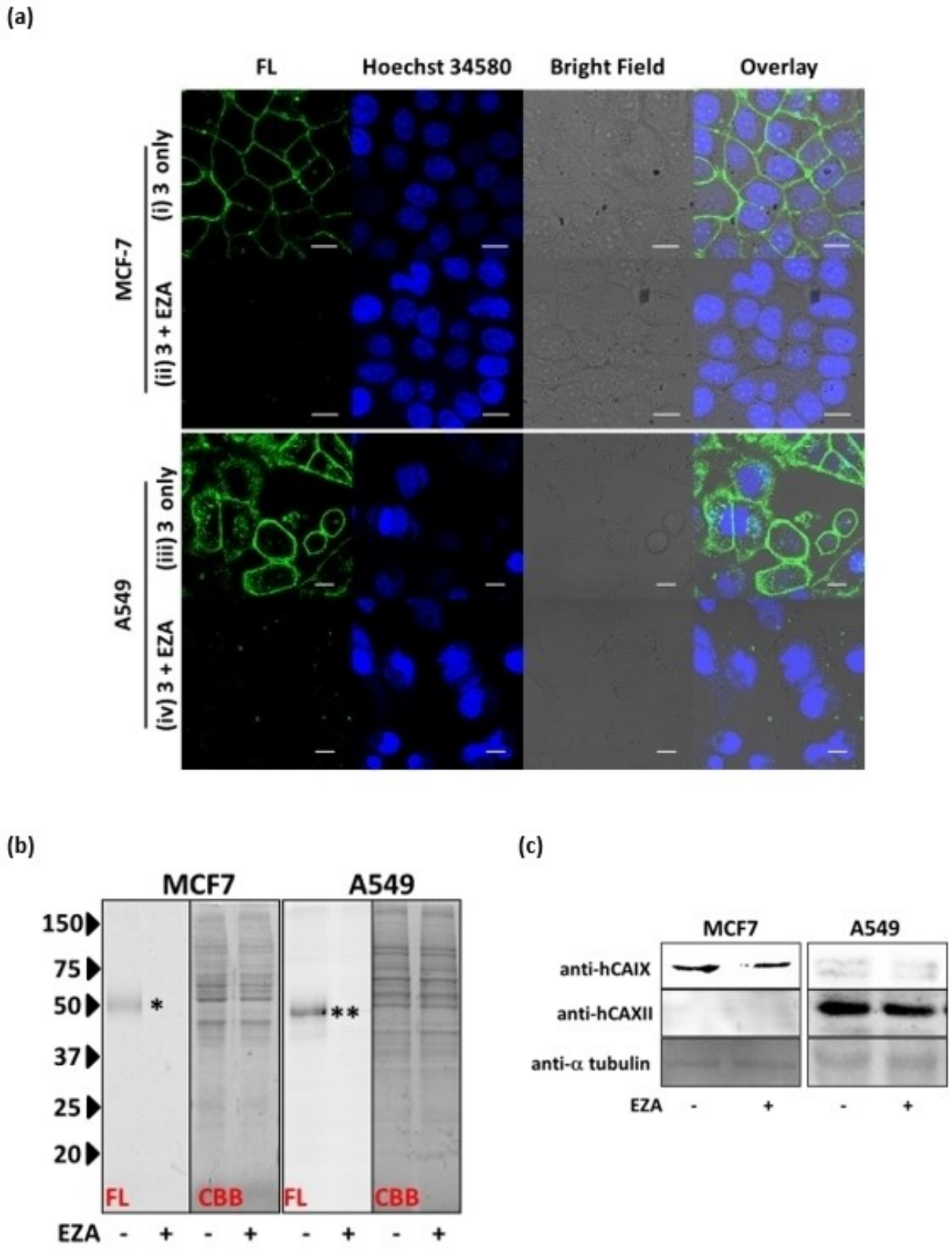

Figure 5. Live-cell imaging of MCF7 and A549 cells expressing endogenous extracellular hCAs. (i) and (iii) were treated with **3** only, while (ii) and (iv) were with **3** and 100 μM EZA. Images were taken after incubating the cells with 5 μM **3** for 2 hours at 37 °C in DMEM medium. Scale bar: 40 μm. (b) SDS-PAGE in-gel fluorescence analyses of the labeling of endogenous hCAs with 5 μM **3** in living MCF7 and A549 cells in the absence or presence of 100 μM EZA. The band with a single asterisk (*) corresponds to hCAIX and the double asterisk (**) corresponds to hCAXII. (c) Western blotting analyses of the endogenous hCAs in living MCF7 and A549 cells, detected with anti-hCAIX and anti-hCAXII antibodies.

© 2021 Wiley-VCH GmbH

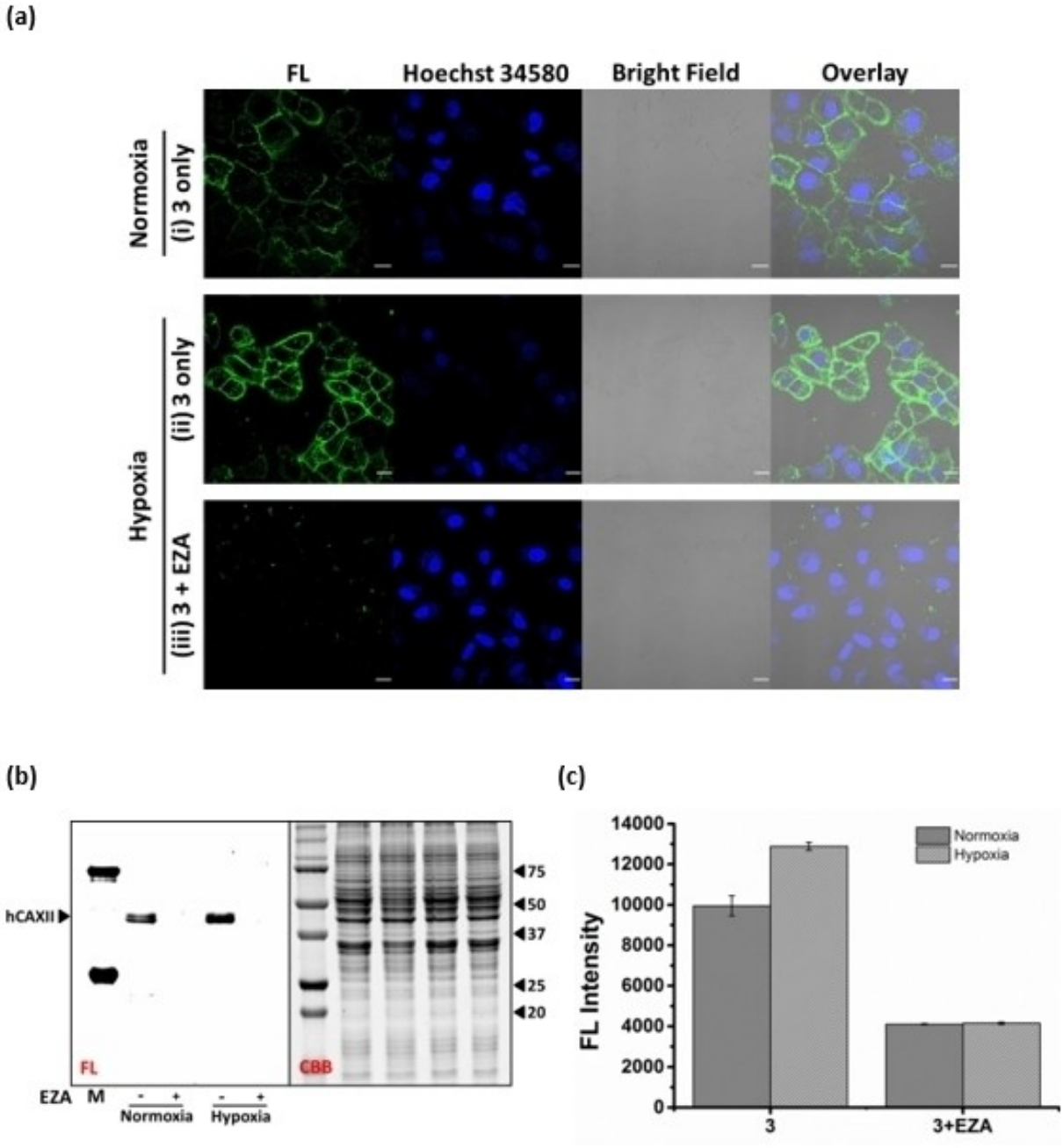

Figure 6. Labeling of normoxia and hypoxia-induced carbonic anhydrase isozymes of A549 cells with **3**. (a) Live cell images of normoxia and hypoxia-induced A549 cells labeled with 5 μM **3** for 2 hours. (i) and (ii) were treated with **3** only while (iii) was treated with **3** and 100 μM EZA. All cellular images were taken on the same day with identical microscope setup. Scale bar: 50 μm. (b) SDS-PAGE in-gel fluorescence analyses of the **3**-labeled A549 cells under normoxia and hypoxia-mimetic conditions and in the absence or presence of EZA inhibitor. M denotes the molecular weight marker with the upper and the lower band corresponding to 75- and 25-KDa, respectively. (c) Quantitative analysis of hCAXII level of A549 cells cultured under normoxia and hypoxia-mimetic conditions. The fluorescent intensity was determined from **3**-labeled hCAXII in-gel image shown in 6b. Error bars were calculated from three independent measurements.

is in accordance with many previous findings.[14d,17] Thus, cell-impermeable **3** and **6** can be harnessed as a new selective and sensitive protein labeling probe to study the expression of different transmembrane hCAs and the results provide the first quantitative data of the level of hCAs under basal and stimulated conditions. Owing to the modular nature of the probe design, we believe that many other extracellular proteins can also be studied by our affinity-based difluorophenyl pivalate probes.

© 2021 Wiley-VCH GmbH

Intracellular endogenous protein labeling using cell-permeable difluorophenyl pivalate probe

To demonstrate that our protein labeling probe design can also be employed to label endogenous intracellular proteins, we converted the cell-impermeable **3** to the permeable form by introducing two acetates to the fluorescein dye to generate **3(OAc)$_2$** (Figure 2a). When 0.5 μM **3(OAc)$_2$** was added to living MCF7 cells and incubated at 37 °C for 3 hours, a strong fluorescence signal was observed in the cytosol as well as on the cell surface (Figure 7a). In contrast, weak fluorescent emission was observed in the presence of ethoxzolamide. We also validated this result by using **3(OAc)$_2$** to label HeLa cells that over-express cytosolic CFP-hCAII protein. The fluorescence from the fluorescein channel overlaid very well with the cytosolic CFP-hCAII protein (Figure S23). To assess the labeling specificity of the probe, the cells labeled with **3(OAc)$_2$** were lysed and analyzed by in-gel fluorescence imaging (Figure 7b). Despite the presence of various other proteins inside the cells, only two distinctive fluorescence bands were observed at around 50 and 30 KDa, corresponding to hCAIX and hCAII proteins, respectively. The two fluorescent bands were sulfonamide-responsive, which were not observed in the presence of EZA inhibitors. It is noteworthy to mention that treatment of the drug-resistant MCF7 cells with Verapamil, an inhibitor of drug efflux pump proteins, was important for the probe to diffuse across the cell membrane. Taken together, these results show that protein modification by difluorophenyl pivalate probes occurs via a specific ligand-protein interaction to label not only extracellular proteins but also intracellular targets with strict specificity in live cells.

In vivo labeling and imaging of tumor cells

Currently, there are many strategies available to achieve in vivo protein labeling. However, almost all of the existing methods require the incorporation of a genetic tag to facilitate protein labeling. Although a protein labeling probe based on tosyl electrophile has been demonstrated previously to achieve in vivo protein modification, the probe can only label the highly abundant hCAII protein of red blood cells in living mice.[18] To date, covalent modification of low abundance endogenous proteins in vivo remains challenging. To this end, we showed that tumor cells expressing endogenous hCAXII protein biomarker in living mice can be successfully labeled by **6**, which were validated by in vivo, ex vivo, and in-gel fluorescence imaging.

Probe **6** was intravenously injected via tail vein into the tumor-bearing mice prepared by subcutaneous inoculation of A549 cells. The fluorescent images in Figure 8a showed the biodistribution of **6** in head, neck, and chest regions at 2, 4, and 24 hours after intravenous injection. By the second hour, the probe remained in the blood circulatory system as observed by the very strong fluorescent signals present in the head, neck, and chest regions of mice. The probe can specifically target either small (top row, 138 mm^3) or large (bottom row, 469 mm^3) subcutaneous tumors developed by A549 cells in the xenograft,

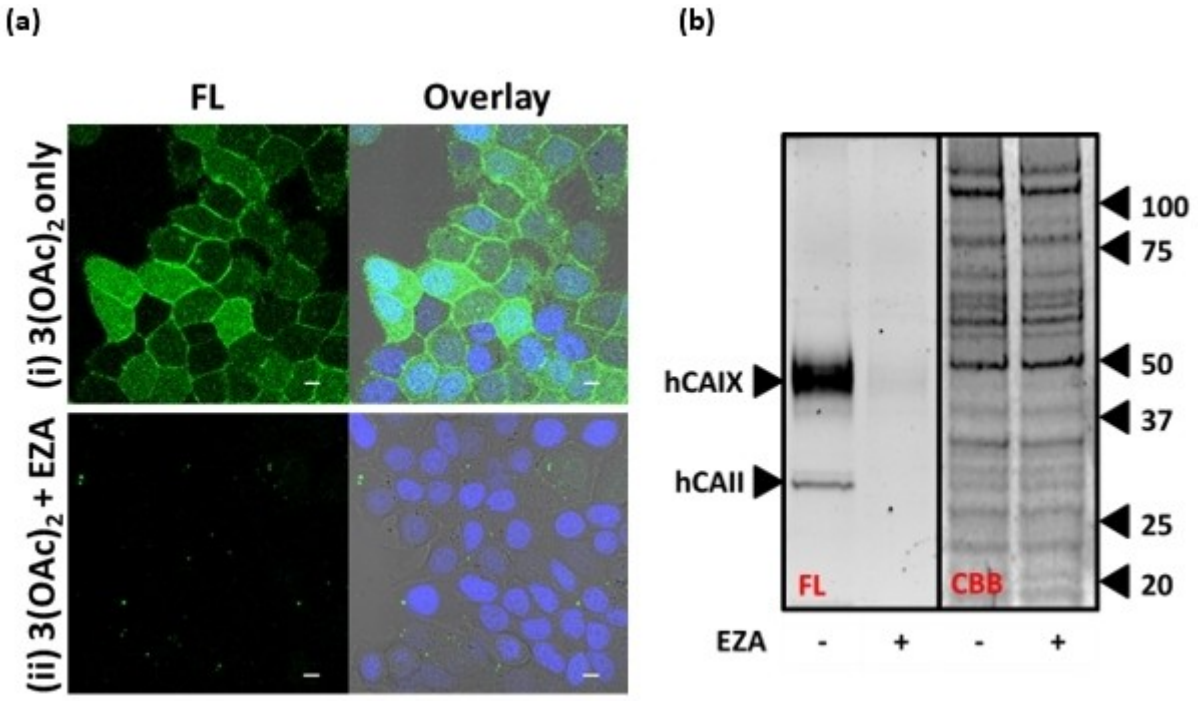

Figure 7. Labeling of endogenous intracellular proteins of MCF7 cells using probe **3(OAc)$_2$**. (a) Images of MCF7 cells after treatment with (i) 0.5 μM **3(OAc)$_2$** for 3 hours at 37 °C in DMEM medium or (ii) in the presence of 100 μM EZA. All cellular images were taken on the same day with identical microscope setup. Scale bar: 20 μm. (b) SDS-PAGE in-gel fluorescence analyses of the labeling of living MCF7 cells with 0.5 μM **3(OAc)$_2$** for 2 hours in the absence or presence of 100 μM EZA. For the labeling of intracellular hCAII, 50 μM Verapamil and **3(OAc)$_2$** were added together to the cells.

© 2021 Wiley-VCH GmbH

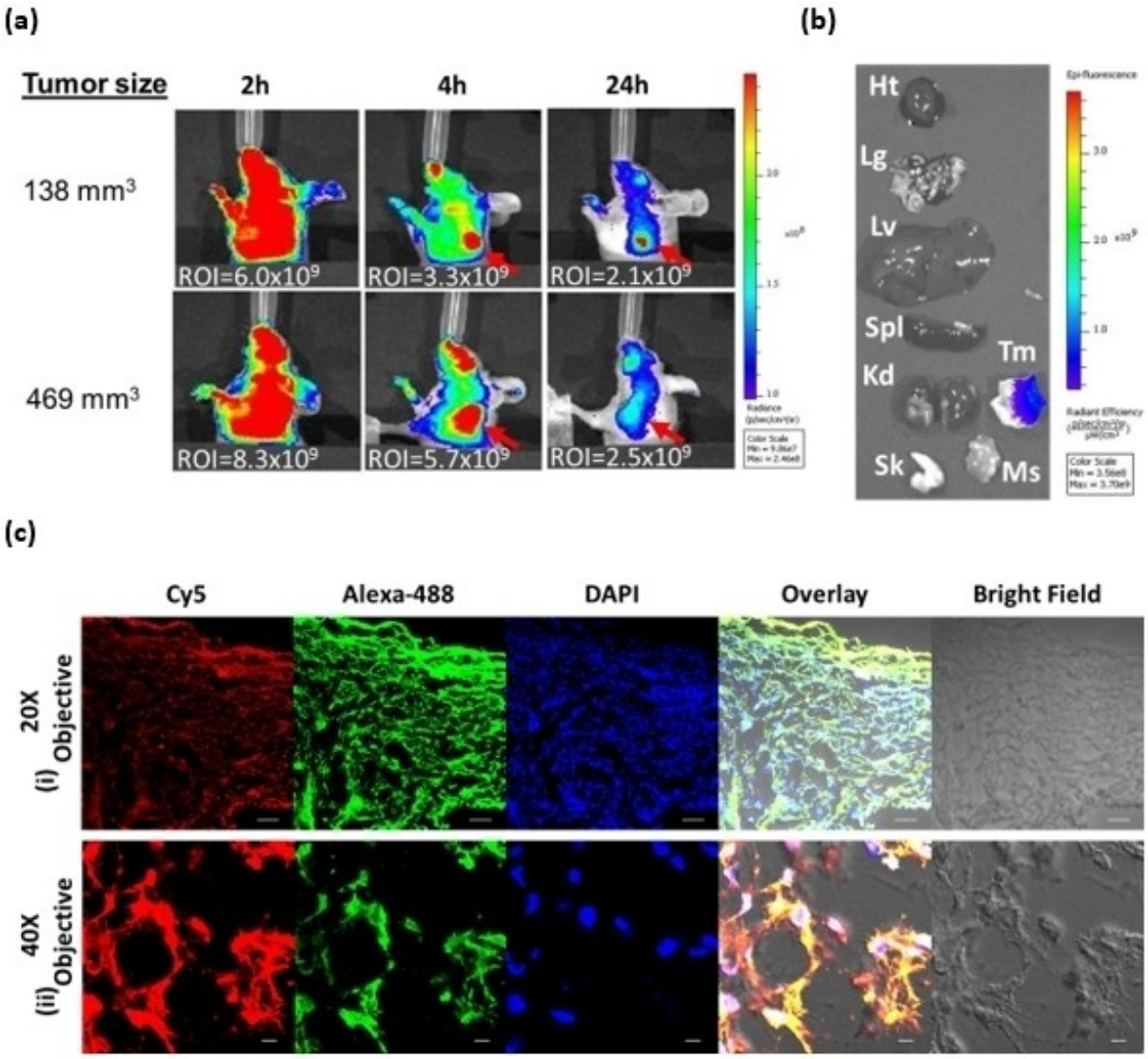

Figure 8. Labeling and imaging of hCAXII in living mice with probe **6**. (a) In vivo imaging and biodistribution of **6** within 24 hours after intravenous injection. Red arrows indicate the accumulation of **6** in A549 tumor. (b) Ex vivo images of tumor, organs, and tissues at the 24 hour after injection of **6**. Abbreviation: Ht (heart), Kd (kidney), Lv (liver), Lg (lung), Spl (spleen), Ms (muscle), Sk (skin), Tm (tumor). (c) Immunohistochemistry staining of the **6**-labeled tumor section by using anti-hCAXII antibody. Images acquired with different magnifications (i) 20x objective, scale bar: 100 μm, (ii) 40x objective, scale bar: 20 μm. The Cy5 of probe **6** are shown in red. The Alexa488 of the antibody are shown in green. The nuclear dye DAPI are shown in blue.

with significant accumulation in the tumor at 4 and 24 hours after injection. By the fourth hour after injection, the apparent difference between the small and large tumors could be observed, where the large tumor presented $>70\%$ elevation of fluorescent signal (5.7×10^9 vs. 3.3×10^9) than the smaller one. 24 hours after injection, there was an approximately 15% increase in the fluorescent signal in the large tumor as compared to that in the smaller tumor, suggesting majority of probe **6** molecules were excreted through mice.

The mice ($N=4$) were sacrificed 24 hours after the injection of **6** to verify the in vivo images. Organs and tissues were collected for ex vivo imaging and the fluorescent intensities were quantified to calculate the biodistribution (Figure 8b). The ex vivo images showed that stronger fluorescent signals were observed in the tumor rather than other organs, such as heart, lung, liver, spleen, kidney, etc. Despite only 0.57% injected dose (ID) presence in the tumor at 24 h (Table S1), the concentration of **6** in the tumor (0.037%ID/g) is significantly higher than that in other tissues and organs except for stomach (0.25%ID/g) and intestine (0.46%ID/g). These results are reasonable because carbonic anhydrase (CA) isozymes are also highly expressed in gastrointestinal mucosa.[19] In contrast to other in vivo imaging probes for CAs, probe **6** also exhibits superior tumor-to-liver (T/L >3.6) and tumor-to-blood (T/B >12) ratios, indicating that the probe is a specific tumor-targeting reagent to image the growth of tumor.[20]

To confirm the in vivo results, an immunohistochemistry experiment was performed by using anti-hCAXII antibody to

© 2021 Wiley-VCH GmbH

stain the tumor section. The results showed that fluorescence from the antibody co-localize very well with the Cy5 signals of probe **6** (Figure 8c). To further validate that the high fluorescence observed in the tumor is due to the covalent modification of hCAXII by probe **6**, the tumor cells were homogenized and analyzed together with **6**-labeled A549 cells by SDS-PAGE in-gel fluorescent imaging (Figure S24). Besides the labeling of high abundance blood proteins: mice serum albumin (SA) and carbonic anhydrase II (CAII), the gel also showed a distinctive 44 KDa fluorescent band from the tumor lysates which was verified by the A549 cell lysates to be the hCAXII protein. These results suggested the ability of **6** to label low abundant target protein in vivo. Thus, the affinity-based protein labeling probes with a sterically stabilized difluorophenyl pivalate electrophile present a novel solution to resist auto and catalytic hydrolysis yet exhibiting sufficient labeling rate to enable protein modification in vivo.

Conclusions

In summary, we have developed a novel affinity-based traceless protein labeling probe approach with high selectivity, stability and sensitivity to label target proteins in complex environments of living cells and in vivo. The probes exhibit long term stability in aqueous buffer and stock solutions, as well as resistance to catalytic hydrolysis by esterase. As compared to all the other protein labeling probes, our probe design features a unique difluorophenyl pivalate as the activated module to accomplish high selectivity, sensitivity and stability. The moderate pKa of difluorophenol ensures the long term stability of the probe in stock solutions and aqueous buffer, while the large steric hindrance provided by the pivalate group imparts resistance to both autolysis and catalytic hydrolysis. The introduction of a large steric effect is crucial for the probe to reduce nonspecific protein labeling which acts by decreasing the reactivity of the activated phenyl ester. Therefore, chemical reaction induced by the proximity effect can only occur via the specific protein-ligand interaction. Owing to the modular design and the versatile synthetic scheme, different fluorophores and ligands can be attached easily on the probes to label various natural (or engineered) proteins having nucleophilic amino acids situated around the ligand binding site, as shown in the cases of avidin, eDHFR and hCAs. With the cell-impermeable sulfonamide probes, we have revealed the major CA proteins expressed on the cell surface of MCF7 and A549 cells to be hCAIX and hCAXII respectively. Furthermore, the in-gel analysis of the 6-labeled tumor lysate also implies that covalent modification of tumor protein in vivo can be achieved with our affinity-based protein labeling probe. We believe that this difluorophenyl pivalate probe approach can spearhead the development of novel protein labeling reagents to become an important tool in drug-discovery, medical diagnosis and basic biology research.

Acknowledgements

We are grateful to the Ministry of Science and Technology (Grant No.: 108-2113-M-007-028-MY3), Ministry of Education ("Aim for the Top University Plan"; Grant No.: 107QR001I5) and National Tsing Hua University (Grant No.: 108QI009E1), for financial support. We also thank Hsin-Ru Wu of the Instrumentation Center of National Tsing Hua University for HRMS measurements.

Conflict of Interest

The authors declare no conflict of interest.

Keywords: Protein labeling · Membrane proteins · Hypoxia · Fluorescent Imaging · Difluorophenyl ester

[1] a) S. Ziegler, V. Pries, C. Hedberg, H. Waldmann, *Angew. Chem. Int. Ed. Engl.* **2013**, *52*, 2744–2792; b) G. Crivat, J. W. Taraska, *Trends Biotechnol.* **2012**, *30*, 8–16; c) K. Tsuchikama, Z. An, *Protein Cell* **2018**, *9*, 33–46.
[2] a) J. Lotze, U. Reinhardt, O. Seitz, A. G. Beck-Sickinger, *Mol. BioSyst.* **2016**, *12*, 1731–1745; b) H.-J. Chen, C. Y. Chew, E.-H. Chang, Y.-W. Tu, L.-Y. Wei, B.-H. Wu, C.-H. Chen, Y.-T. Yang, S.-C. Huang, J.-K. Chen, I. C. Chen, K.-T. Tan, *J. Am. Chem. Soc.* **2018**, *140*, 5224–5234; c) C. Jing, V. W. Cornish, *Acc. Chem. Res.* **2011**, *44*, 784–792; d) C. D. Spicer, B. G. Davis, *Nat. Commun.* **2014**, *5*, 4740.
[3] a) T. Tamura, I. Hamachi, *J. Am. Chem. Soc.* **2019**, *141*, 2782–2799; b) D. P. Murale, S. C. Hong, M. M. Haque, J.-S. Lee, *Proteome Sci.* **2017**, *15*, 14; c) C. G. Parker, A. Galmozzi, Y. Wang, B. E. Correia, K. Sasaki, C. M. Joslyn, A. S. Kim, C. L. Cavallaro, R. M. Lawrence, S. R. Johnson, I. Narvaiza, E. Saez, B. F. Cravatt, *Cell* **2017**, *168*, 527–541.e529; d) Y.-C. Chen, K. M. Backus, M. Merkulova, C. Yang, D. Brown, B. F. Cravatt, C. Zhang, *J. Am. Chem. Soc.* **2017**, *139*, 639–642.
[4] a) T. Tamura, Y. Kioi, T. Miki, S. Tsukiji, I. Hamachi, *J. Am. Chem. Soc.* **2013**, *135*, 6782–6785; b) T. Miki, S.-H. Fujishima, K. Komatsu, K. Kuwata, S. Kiyonaka, I. Hamachi, *Chem. Biol.* **2014**, *21*, 1013–1022; c) Y. Takaoka, Y. Nishikawa, Y. Hashimoto, K. Sasaki, I. Hamachi, *Chem. Sci.* **2015**, *6*, 3217–3224; d) K. Matsuo, Y. Nishikawa, M. Masuda, I. Hamachi, *Angew. Chem. Int. Ed.* **2018**, *57*, 659–662; *Angew. Chem.* **2018**, *130*, 667–670; e) T. Tamura, T. Ueda, T. Goto, T. Tsukidate, Y. Shapira, Y. Nishikawa, A. Fujisawa, I. Hamachi, *Nat. Commun.* **2018**, *9*, 1870.
[5] a) A. F. Kornahrens, A. B. Cognetta, D. M. Brody, M. L. Matthews, B. F. Cravatt, D. L. Boger, *J. Am. Chem. Soc.* **2017**, *139*, 7052–7061; b) S. M. Hacker, K. M. Backus, M. R. Lazear, S. Forli, B. E. Correia, B. F. Cravatt, *Nat. Chem.* **2017**, *9*, 1181; c) S. Tsukiji, H. Wang, M. Miyagawa, T. Tamura, Y. Takaoka, I. Hamachi, *J. Am. Chem. Soc.* **2009**, *131*, 9046–9054; d) M. H. Wright, S. A. Sieber, *Nat. Prod. Rep.* **2016**, *33*, 681–708; e) B. D. Horning, R. M. Suciu, D. A. Ghadiri, O. A. Ulanovskaya, M. L. Matthews, K. M. Lum, K. M. Backus, S. J. Brown, H. Rosen, B. F. Cravatt, *J. Am. Chem. Soc.* **2016**, *138*, 13335–13343; f) J. S. Marvin, H. W. Hellinga, *J. Am. Chem. Soc.* **1998**, *120*, 7–11.
[6] a) C. C. Hughes, Y.-L. Yang, W.-T. Liu, P. C. Dorrestein, J. J. L. Clair, W. Fenical, *J. Am. Chem. Soc.* **2009**, *131*, 12094–12096; b) H.-J. Chan, X.-H. Lin, S.-Y. Fan, J. Ru Hwu, K.-T. Tan, *Chem. Asian J.* **2020**, *15*, 3416–3420.
[7] J. Han, F.-M. Tao, *J. Phys. Chem. A* **2006**, *110*, 257–263.
[8] V. M. Krishnamurthy, G. K. Kaufman, A. R. Urbach, I. Gitlin, K. L. Gudiksen, D. B. Weibel, G. M. Whitesides, *Chem. Rev.* **2008**, *108*, 946–1051.
[9] a) M. E. Olson, D. Abate-Pella, A. L. Perkins, M. Li, M. A. Carpenter, A. Rathore, R. S. Harris, D. A. Harki, *J. Med. Chem.* **2015**, *58*, 7419–7430; b) Z. Blaxill, S. Holland-Crimmin, R. Lifely, *J. Biomol. Screening* **2009**, *14*, 547–556.
[10] a) O. Koniev, A. Wagner, *Chem. Soc. Rev.* **2015**, *44*, 5495–5551; b) G. T. Hermanson, *Bioconjugate Techniques*, Elsevier Science, **2013**.
[11] L. D. Lavis, T.-Y. Chao, R. T. Raines, *Chem. Sci.* **2011**, *2*, 521–530.
[12] Craig S. McKay, M. G. Finn, *Chem. Biol.* **2014**, *21*, 1075–1101.
[13] a) X. Tan, Z. Song, *RSC Adv.* **2014**, *4*, 3263–3271; b) R. Zini, P. d'Athis, A. Hoareau, J. P. Tillement, *Eur. J. Clin. Pharmacol.* **1976**, *10*, 139–145.

© 2021 Wiley-VCH GmbH

[14] a) J. Chiche, K. Ilc, J. Laferrière, E. Trottier, F. Dayan, N. M. Mazure, M. C. Brahimi-Horn, J. Pouysségur, *Cancer Res.* **2009**, *69*, 358–368; b) J. Jiang, J. H. Zhao, X. L. Wang, X. J. Guo, J. Yang, X. Bai, S. Y. Jin, R. L. Ge, *Neoplasma* **2015**, *62*, 456–463; c) Z. Chen, L. Ai, M. Y. Mboge, C. Tu, R. McKenna, K. D. Brown, C. D. Heldermon, S. C. Frost, *PLoS One* **2018**, *13*, e0199476; d) C. C. Wykoff, N. J. P. Beasley, P. H. Watson, K. J. Turner, J. Pastorek, A. Sibtain, G. D. Wilson, H. Turley, K. L. Talks, P. H. Maxwell, C. W. Pugh, P. J. Ratcliffe, A. L. Harris, *Cancer Res.* **2000**, *60*, 7075–7083.
[15] a) C. T. Supuran, *Nat. Rev. Drug Discovery* **2008**, *7*, 168; b) A. Nógrádi, *Am. J. Pathol.* **1998**, *153*, 1–4; c) P. H. Watson, S. K. Chia, C. C. Wykoff, C. Han, R. D. Leek, W. S. Sly, K. C. Gatter, P. Ratcliffe, A. L. Harris, *Br. J. Cancer* **2003**, *88*, 1065–1070.
[16] a) Y. Yuan, G. Hilliard, T. Ferguson, D. E. Millhorn, *J. Biol. Chem.* **2003**, *278*, 15911–15916; b) D. Wu, P. Yotnda, *J. Visualization* **2011**, 2899.
[17] M. Ilie, V. Hofman, J. Zangari, J. Chiche, J. Mouroux, N. M. Mazure, J. Pouysségur, P. Brest, P. Hofman, *Lung Cancer* **2013**, *82*, 16–23.
[18] S. Tsukiji, M. Miyagawa, Y. Takaoka, T. Tamura, I. Hamachi, *Nat. Chem. Biol.* **2009**, *5*, 341.
[19] a) T. Kleinke, S. Wagner, H. John, D. Hewett-Emmett, S. Parkkila, W.-G. Forssmann, G. Gros, *J. Exp. Biol.* **2005**, *208*, 487–496; b) V. Endeward, T. Kleinke, G. Gros, *Comp. Biochem. Physiol., Part A Mol. Integr. Physiol.* **2003**, *136*, 281–287; c) R. E. Fleming, S. Parkkila, A. K. Parkkila, H. Rajaniemi, A. Waheed, W. S. Sly, *J. Clin. Invest.* **1995**, *96*, 2907–2913; d) S.-i. Igarashi, Y. Kano, T. Nishita, H. Amasaki, M. Asari, *J. Vet. Med. Sci.* **1992**, *54*, 535–539.
[20] a) B. Bao, K. Groves, J. Zhang, E. Handy, P. Kennedy, G. Cuneo, C. T. Supuran, W. Yared, M. Rajopadhye, J. D. Peterson, *PLoS One* **2012**, *7*, e50860; b) J. Lau, Z. Liu, K. S. Lin, J. Pan, Z. Zhang, D. Vullo, C. T. Supuran, D. M. Perrin, F. Benard, *J. Nucl. Med.* **2015**, *56*, 1434–1440.

Manuscript received: January 19, 2021
Revised manuscript received: February 23, 2021
Accepted manuscript online: February 25, 2021
Version of record online: March 9, 2021

© 2021 Wiley-VCH GmbH